Available online at www.sciencedirect.com
ScienceDirect
Journal of Sound and Vibration 312 (2008) 563–571
JOURNAL OF SOUND AND VIBRATION
www.elsevier.com/locate/jsvi

Rapid Communication

A modified transfer matrix method for the coupled lateral and torsional vibrations of asymmetric rotor-bearing systems

Sheng-Chung Hsieh[a], Juhn-Horng Chen[b], An-Chen Lee[a,*]

[a]*Department of Mechanical Engineering, National Chiao Tung University, 1001 Ta Hsueh Road, Hsinchu 30049, Taiwan, ROC*
[b]*Department of Mechanical Engineering, Chung Hua University, Taiwan, ROC*

Received 23 September 2007; received in revised form 30 November 2007; accepted 4 January 2008
Handling Editor: L.G. Tham

Abstract

For analyzing the coupled lateral and torsional vibrations of asymmetric rotor-bearing system, an extended transfer matrix extended from one of the symmetric system is developed. Rather than the conventional ''lumped system'', the asymmetric rotating shaft is modeled by the Timoshenko beam in a continuous-system concept. According to our analysis, for the asymmetric isotropic rotor-bearing system, the synchronous lateral mode will split; moreover, there is a $2\times$ lateral mode that does not appear on symmetric isotropic rotor-bearing systems.

1. Introduction

Schwibinger and Nordmann [1] investigated the influence of torsional–lateral coupling on the stability behavior of a simple geared system supported by oil film bearings. Qin and Mao [2] developed a new finite element model for analyzing the torsional–flexural characteristics of the rotor system. Additionally, Rao et al. [3] studied the lateral transient response of geared rotors raised by torsional excitation. Mohiuddin and Khulief [4] developed a reduced modal form of the rotor-bearing system for finding the transient responses owing to different excitations using the finite element method. Al-Bedoor [5] presented a dynamic model for a typical elastic blade attached to a disk mounted on a shaft, which was flexible in the torsional direction. Additionally, Al-Bedoor [6] presented a model for interpreting the coupled torsional and lateral transient vibrations of the simple Jeffcott rotor. Lee [7] formulated the coupled equations of motion in a lateral bending-torsion for an unbalanced disk of the simple Jeffcott rotor for analyzing the instabilities. Hsieh et al. [8] developed a modified transfer matrix method for analyzing the coupled lateral and torsional vibrations of the symmetric rotor-bearing system with an external perturbing torque.

This paper extends the work of Hsieh et al. [8] and offers a modified transfer matrix method for analyzing the coupled lateral and torsional vibrations of asymmetric rotor-bearing systems with an external perturbing torque.

*Corresponding author. Tel.: +886 3 5728513; fax: +886 3 5725372.
E-mail address: aclee@cc.nctu.edu.tw (A.-C. Lee).

0022-460X/$ - see front matter © 2008 Elsevier Ltd. All rights reserved.
doi:10.1016/j.jsv.2008.01.006

2. Transfer matrix of Timoshenko's shaft

Considering the kinetic energy and potential energy of the asymmetric shaft element expressed in fixed coordinates [8,9], using Hamilton's principle and assuming small twist angle displacement, we know that the force equilibrium equations of the asymmetric shaft in the fixed coordinates can be obtained as follows:

$$\begin{aligned}&\rho A[\ddot{\varphi}e_v^s\cos(\Omega t+\varphi+\beta_1^s)+\ddot{\varphi}e_u^s\sin(\Omega t+\varphi+\beta_1^s)-(\Omega+\dot{\varphi})^2e_v^s\sin(\Omega t+\varphi+\beta_1^s)\\&\quad+(\Omega+\dot{\varphi})^2e_u^s\cos(\Omega t+\varphi+\beta_1^s)]-\rho A\ddot{x}+k_sGA(x''-\theta_y')=0,\end{aligned}\tag{1}$$

$$\begin{aligned}&\rho A[-\ddot{\varphi}e_u^s\cos(\Omega t+\varphi+\beta_1^s)+\ddot{\varphi}e_v^s\sin(\Omega t+\varphi+\beta_1^s)+(\Omega+\dot{\varphi})^2e_u^s\sin(\Omega t+\varphi+\beta_1^s)\\&\quad+(\Omega+\dot{\varphi})^2e_v^s\cos(\Omega t+\varphi+\beta_1^s)]-\rho A\ddot{y}+k_sGA(\theta_x'+y'')-\rho Ag=0,\end{aligned}\tag{2}$$

where A, ρ, G and k_s denote the cross-sectional area, density, shear modulus and Timoshenko's shear coefficient, respectively, x and y denote the deflections of the geometric center in X and Y directions, respectively, θ_x and θ_y denote the angular displacements in X and Y directions, respectively, e_u^s and e_v^s denote the components of the eccentricity in U, V directions [8], respectively, φ and Ω denote the angle of twist and rotating speed, respectively, β_1^s denotes the initial angle between the principal axes U and X [8].

The bending moment equilibrium equations in the fixed coordinates are

$$\begin{aligned}&\rho I^s\ddot{\theta}_x+\frac{1}{2}\rho I_p^s\ddot{\varphi}\theta_y+\rho I_p^s(\Omega+\dot{\varphi})\dot{\theta}_y-EI^s\theta_x''+k_sGA(\theta_x+y')+\rho\Delta^s[\ddot{\theta}_y\sin 2(\Omega t+\varphi+\beta_1^s)\\&\quad+2\dot{\theta}_y(\Omega+\dot{\varphi})\cos 2(\Omega t+\varphi+\beta_1^s)+\ddot{\theta}_x\cos 2(\Omega t+\varphi+\beta_1^s)-2\dot{\theta}_x(\Omega+\dot{\varphi})\sin 2(\Omega t+\varphi+\beta_1^s)]\\&\quad+E\Delta^s[-\theta_y''\sin 2(\Omega t+\varphi+\beta_1^s)-2\theta_y'\varphi'\cos 2(\Omega t+\varphi+\beta_1^s)-\theta_x''\cos 2(\Omega t+\varphi+\beta_1^s)\\&\quad+2\theta_x'\varphi'\sin 2(\Omega t+\varphi+\beta_1^s)]=0,\end{aligned}\tag{3}$$

$$\begin{aligned}&\rho I^s\ddot{\theta}_y-\tfrac{1}{2}\rho I_p^s\ddot{\varphi}\theta_x-\rho I_p^s(\Omega+\dot{\varphi})\dot{\theta}_x-EI^s\theta_y''+k_sGA(\theta_y-x')+\rho\Delta^s[\ddot{\theta}_x\sin 2(\Omega t+\varphi+\beta_1^s)\\&\quad+2\dot{\theta}_x(\Omega+\dot{\varphi})\cos 2(\Omega t+\varphi+\beta_1^s)-\ddot{\theta}_y\cos 2(\Omega t+\varphi+\beta_1^s)+2\dot{\theta}_y(\Omega+\dot{\varphi})\sin 2(\Omega t+\varphi+\beta_1^s)]\\&\quad+E\Delta^s[-\theta_x''\sin 2(\Omega t+\varphi+\beta_1^s)-2\theta_x'\varphi'\cos 2(\Omega t+\varphi+\beta_1^s)+\theta_y''\cos 2(\Omega t+\varphi+\beta_1^s)\\&\quad-2\theta_y'\varphi'\sin 2(\Omega t+\varphi+\beta_1^s)]=0,\end{aligned}\tag{4}$$

where I^s, Δ^s and $I^s{}_p$ denote the mean, deviatoric and polar area moment of inertia [8], respectively, E denotes Young's modulus.

The torque equilibrium equation in the fixed coordinates is

$$\begin{aligned}&\rho I_p^s\ddot{\varphi}-GI_p^s\varphi''+\tfrac{1}{2}\rho I_p^s(\ddot{\theta}_x\theta_y-\ddot{\theta}_y\theta_x)+\rho A[-\ddot{x}e_v^s\cos(\Omega t+\varphi+\beta_1^s)-\ddot{x}e_u^s\sin(\Omega t+\varphi+\beta_1^s)\\&\quad+\ddot{y}e_u^s\cos(\Omega t+\varphi+\beta_1^s)-\ddot{y}e_v^s\sin(\Omega t+\varphi+\beta_1^s)+(e^s)^2\ddot{\varphi}]+\rho\Delta^s[-2\dot{\theta}_x\dot{\theta}_y\cos 2(\Omega t+\varphi+\beta_1^s)\\&\quad+(\dot{\theta}_x)^2\sin 2(\Omega t+\varphi+\beta_1^s)-(\dot{\theta}_y)^2\sin 2(\Omega t+\varphi+\beta_1^s)]+E\Delta^s[+2\theta_x'\theta_y'\cos 2(\Omega t+\varphi+\beta_1^s)\\&\quad-(\theta_x')^2\sin 2(\Omega t+\varphi+\beta_1^s)+(\theta_y')^2\sin 2(\Omega t+\varphi+\beta_1^s)]=0.\end{aligned}\tag{5}$$

The natural boundary conditions are

$$\begin{aligned}&V_x+[k_sGA(\theta_y-x')]=0,\quad V_y+[-k_sGA(\theta_x+y')]=0,\quad T+[-GI_P\varphi']=0,\\&M_x+[-EI\theta_x'-E\Delta^s\theta_x'\cos 2(\Omega t+\varphi+\beta_1^s)-E\Delta^s\theta_y'\sin 2(\Omega t+\varphi+\beta_1^s)]=0,\\&M_y+[-EI\theta_y'+E\Delta^s\theta_y'\cos 2(\Omega t+\varphi+\beta_1^s)-E\Delta^s\theta_x'\sin 2(\Omega t+\varphi+\beta_1^s)]=0,\end{aligned}\tag{6}$$

where V_x and V_y denote the shear forces in X and Y directions, respectively, M_x and M_y denote the bending moments in X and Y directions, respectively, T denotes the perturbing axial torque.

If the deviatoric area moment Δ^s is zero, Eqs. (1)–(5) and Eq. (6) are simplified into the equilibrium equations and natural boundary conditions of the symmetric shaft, respectively [8].

Using the same procedure illustrated in Ref. [8], one can construct the shaft transfer matrix $[T^s]$, relating two sides of the asymmetric Timoshenko shaft for the static deflection, synchronous whirl, and $n\times$ (n times the rotating speed) whirl, in the static frame.

3. Transfer matrix of the rigid disk

Assuming the disk is rigid, thin, and asymmetric, one gets the force equilibrium equations of the asymmetric disk in the fixed coordinates:

$$V_x^R - V_x^L + m^d[-\ddot{x} + \ddot{\varphi}e_v^d\cos(\Omega t+\varphi+\beta_1^d) + \ddot{\varphi}e_u^d\sin(\Omega t+\varphi+\beta_1^d) - (\Omega+\dot{\varphi})^2 e_v^d\sin(\Omega t+\varphi+\beta_1^d) + (\Omega+\dot{\varphi})^2 e_u^d\cos(\Omega t+\varphi+\beta_1^d)] = 0, \tag{7}$$

$$V_y^R - V_y^L + m^d[-\ddot{y} - \ddot{\varphi}e_u^d\cos(\Omega t+\varphi+\beta_1^d) + \ddot{\varphi}e_v^d\sin(\Omega t+\varphi+\beta_1^d) + (\Omega+\dot{\varphi})^2 e_u^d\sin(\Omega t+\varphi+\beta_1^d) + (\Omega+\dot{\varphi})^2 e_v^d\cos(\Omega t+\varphi+\beta_1^d)] - w^d = 0, \tag{8}$$

where m^d and w^d denote the mass and weight, respectively, e_u^d and e_v^d denote the components of the eccentricity in U, V directions, respectively, V_x^R and V_x^L denote the shear forces in X direction acting on right and left sides of the disk, respectively, V_y^R and V_y^L denote the shear forces in Y direction acting on right and left sides of the disk, respectively, β_1^d denotes the initial angle between the principal axes U and X.

The bending moment equilibrium equations in the fixed coordinates are

$$M_x^R - M_x^L - I^d\ddot{\theta}_x - \tfrac{1}{2}I_p^d\ddot{\varphi}\theta_y - I_p^d(\Omega+\dot{\varphi})\dot{\theta}_y - \Delta^d\ddot{\theta}_y\sin 2(\Omega t+\varphi+\beta_1^d) - \Delta^d\ddot{\theta}_x\cos 2(\Omega t+\varphi+\beta_1^d) - 2\Delta^d\dot{\theta}_y(\Omega+\dot{\varphi})\cos 2(\Omega t+\varphi+\beta_1^d) + 2\Delta^d\dot{\theta}_x(\Omega+\dot{\varphi})\sin 2(\Omega t+\varphi+\beta_1^d) = 0, \tag{9}$$

$$M_y^R - M_y^L - I^d\ddot{\theta}_y + \tfrac{1}{2}I_p^d\ddot{\varphi}\theta_x + I_p^d(\Omega+\dot{\varphi})\dot{\theta}_x - \Delta^d\ddot{\theta}_x\sin 2(\Omega t+\varphi+\beta_1^d) + \Delta^d\ddot{\theta}_y\cos 2(\Omega t+\varphi+\beta_1^d) - 2\Delta^d\dot{\theta}_x(\Omega+\dot{\varphi})\cos 2(\Omega t+\varphi+\beta_1^d) - 2\Delta^d\dot{\theta}_y(\Omega+\dot{\varphi})\sin 2(\Omega t+\varphi+\beta_1^d) = 0, \tag{10}$$

where I^d, Δ^d and I_p^d denote the mean, deviatoric and polar mass moment of inertia [8], respectively, M_x^R and M_x^L denote the bending moments in X direction acting on right and left sides of the disk, respectively, M_y^R and M_y^L denote the bending moments in Y direction acting on right and left sides of the disk, respectively.

The torque equilibrium equations in the fixed coordinates is

$$T^R - T^L - I_p^d\ddot{\varphi} - \tfrac{1}{2}I_p^d\ddot{\theta}_x\theta_y + \tfrac{1}{2}I_p^d\ddot{\theta}_y\theta_x + m^d[\ddot{x}e_v^d\cos(\Omega t+\varphi+\beta_1^d) + \ddot{x}e_u^d\sin(\Omega t+\varphi+\beta_1^d) - \ddot{y}e_u^d\cos(\Omega t+\varphi+\beta_1^d) + \ddot{y}e_v^d\sin(\Omega t+\varphi+\beta_1^d) - (e^d)^2\ddot{\varphi}] + 2\Delta^d\dot{\theta}_x\dot{\theta}_y\cos 2(\Omega t+\varphi+\beta_1^d) - \Delta^d\dot{\theta}_x^2\sin 2(\Omega t+\varphi+\beta_1^d) + \Delta^d\dot{\theta}_y^2\sin 2(\Omega t+\varphi+\beta_1^d) = 0, \tag{11}$$

where e^d denotes the eccentricity, T^R and T^L denote the axial torque perturbation acting on right and left sides of the disk, respectively.

Similarly, Eqs. (7)–(11) can be simplified into the equilibrium equations of the symmetric disk in Ref. [8] by setting $\Delta^d = 0$.

In this paper, the defections are assumed very small. Therefore, the order of magnitude of the high-order nonlinear terms, such as $\dot{\varphi}^2$, $\ddot{\varphi}\theta_y$, $\dot{\varphi}\dot{\theta}_y$, which involve square term or multiplication term, are quite small and can be ignored, for simplification. Expressing the steady-state responses and inputs in Fourier series forms and substituting them into Eqs. (7)–(11) and equating the coefficients of the same harmonic term can yield the transfer matrix of the disk $[T^d]$ for static, synchronous whirl and non-synchronous whirls in the static frame.

The overall transfer matrix of the rotor system is the relation between the two ends of the shaft, and can be derived by a stepwise relationship of the state vectors from the left end to the right end, and the state variables of other stages are obtained by multiplying transfer matrices from stage 0 of the left end stepwise until a specific stage is reached [8].

4. Numerical example

For comparison, we introduce the same isotropic rotor-bearing system shown in Ref. [8] except that the flexible shaft is asymmetric (Fig. 1). Table 1 lists the relative details of this asymmetric isotropic rotor-bearing system. The response amplitudes and whirling orbits when no external perturbing torque, only the unbalance force and weight acting in the system are shown in Fig. 2. Comparing the results in Ref. [8] with those in Fig. 2, due to the effect of the asymmetric shaft, one gets that the synchronous lateral mode will split and the $2\times$ lateral mode appears additionally. In a rotating coordinates fixed to the asymmetric shaft, the weight can be considered as a $1\times$ external force, which can excite $1\times$ forward whirl and $1\times$ backward whirl due to the effect of the haft asymmetry. In other words, the weight will excite $2\times$ forward whirl and static deflection with

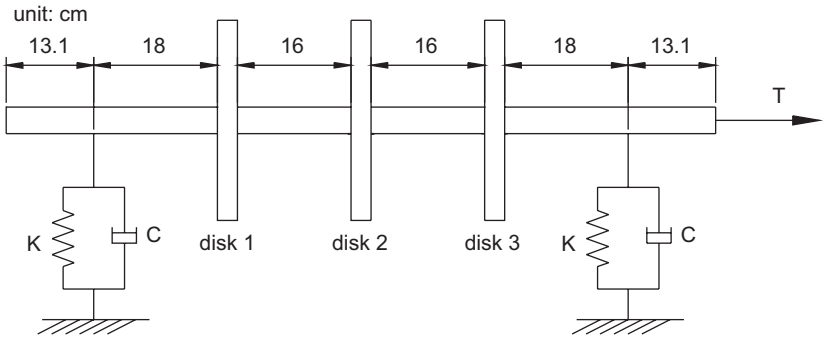

Fig. 1. Configuration of the asymmetric isotropic rotor-bearing system.

Table 1
Details of the asymmetric isotropic rotor-bearing system

The coefficients of the shaft	
A	$1.2566\times10^{-3}\,\mathrm{m}^2$
I_u^s	$1.3823\times10^{-7}\,\mathrm{m}^4$
I_v^s	$1.1309733\times10^{-7}\,\mathrm{m}^4$
E	$207\times10^{9}\,\mathrm{N\,m}^{-2}$
G	$81\times10^{9}\,\mathrm{N\,m}^{-2}$
k_s	0.68
ρ	$7750\,\mathrm{kg\,m}^{-3}$
e_u^s, e_v^s	$1\times10^{-6}\,\mathrm{m}$
β_1^s	0
The coefficients of the disks	
m^d	2.5 kg
I_p^d	$1020\times10^{-4}\,\mathrm{kg\,m}^2$
I_u^d, I_v^d	$512\times10^{-4}\,\mathrm{kg\,m}^2$
e_u^d, e_v^d of the disk 1	$7\times10^{-6}\,\mathrm{m}$
e_u^d, e_v^d of the disk 2 and disk 3	0
β_1^d of the disk1, disk 2 and disk 3	0
The coefficients of the bearings	
K_{xx}, K_{yy}	$1\times10^{7}\,\mathrm{N\,m}^{-1}$
K_{xy}, K_{yx}, $K_{\theta xx}$, $K_{\theta yy}$, $K_{\theta xy}$, $K_{\theta yx}$	0
K_φ of the left bearing	$5\times10^{8}\,\mathrm{N\,m\,rad}^{-1}$
K_φ of the right bearing	0
C_{xx}, C_{yy}	$2\times10^{3}\,\mathrm{N\,s\,m}^{-1}$
C_{xy}, C_{yx}, $C_{\theta xx}$, $C_{\theta yy}$, $C_{\theta xy}$, $C_{\theta yx}$	0
C_φ of the left bearing	$1\,\mathrm{N\,m\,s\,rad}^{-1}$
C_φ of the right bearing	0

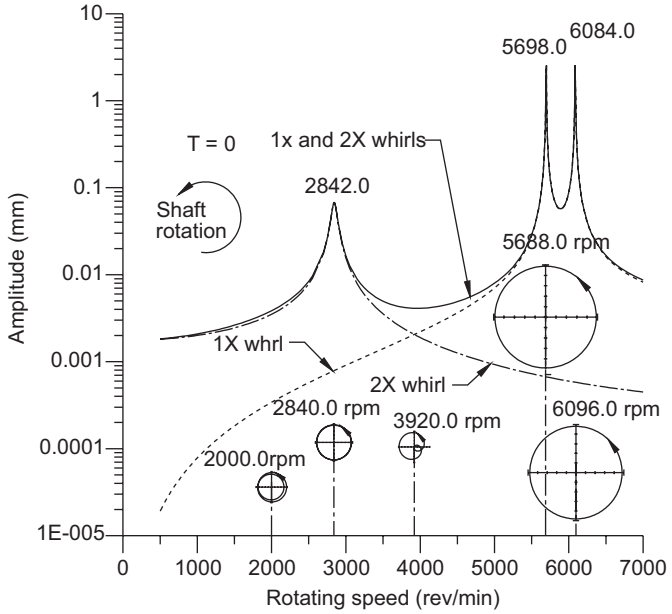

Fig. 2. Response amplitudes and orbits of disk 1 (without perturbing torque).

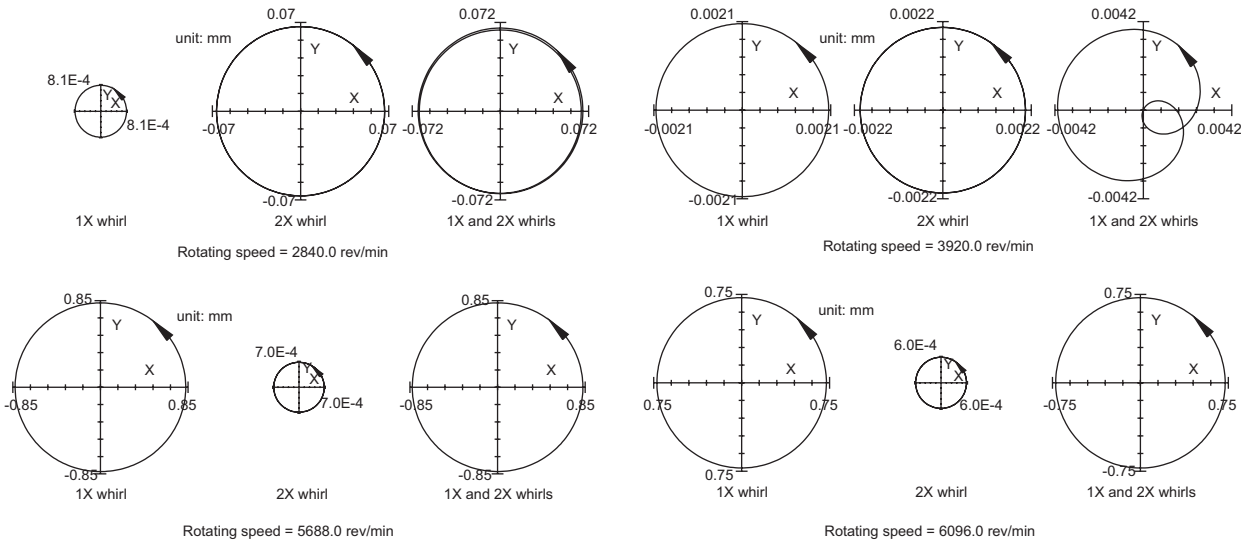

Fig. 3. Whirling orbits of disk 1 (without perturbing torque).

respect to the static frame. Moreover, the critical speed due to the weight is roughly equal to half the critical speed due to the mass unbalance. The synchronous whirl is excited by unbalance force and the $2\times$ whirl is excited by the weight. Two synchronous lateral modes occur at 5698 and 6084 rev/min, respectively, and the $2\times$ lateral mode occurs at 2842 rev/min. The response is composed of synchronous (i.e., $1\times$) and $2\times$ whirls. The synchronous whirl is excited by unbalance force and the $2\times$ whirl is excited by the weight. Fig. 3 shows the orbits of the $1\times$, $2\times$, and synthetic whirls. The orbits of the $1\times$ and $2\times$ components are all forward and right circular so that the synthetic orbit is forward too.

Fig. 4 illustrates the response amplitudes and the orbits of disk 1 excited by the $1\times$ perturbing torque ($T = 5000\cos\Omega t$ N m) along with unbalance force and weight. Other than synchronous and $2\times$ lateral modes,

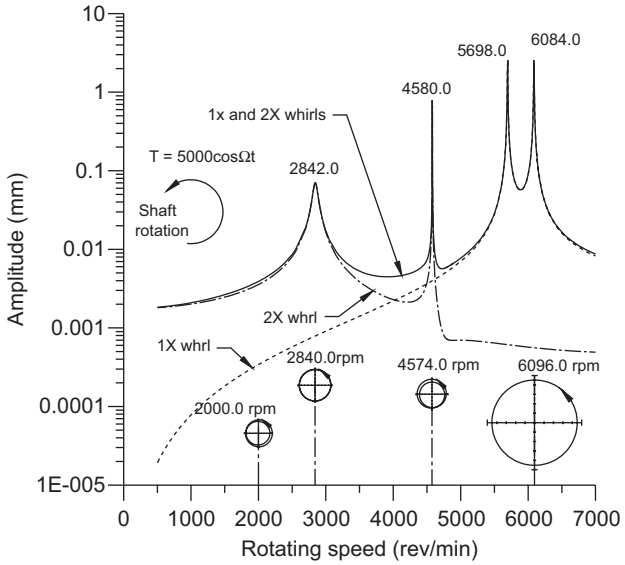

Fig. 4. Response amplitudes and orbits of disk 1 ($T = 5000\cos\Omega t$).

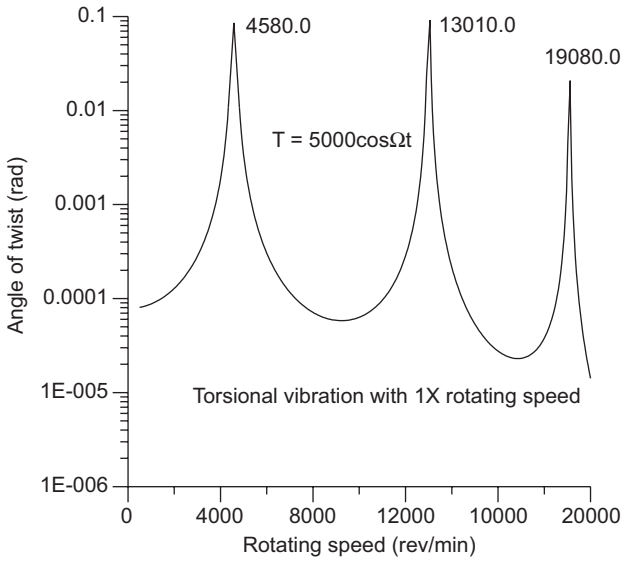

Fig. 5. Angle of twist of disk 1 ($T = 5000\cos\Omega t$).

one peak clearly appears at 4580 rev/min. The response amplitude of the angle of twist of disk 1 is shown in Fig. 5. Like the symmetric isotropic rotor-bearing system [8], the torque will excite the torsional vibration with torsional exciting frequency and, under the system coupling effect, also stimulate the lateral vibration whose frequency is that of the perturbing torque plus or minus the rotating speed. Therefore, owing to the coupling effect of the rotor system, the $1\times$ torque excites a $1\times$ torsional mode at 4580 rev/min, a $2\times$ lateral mode at 2842 rev/min. Fig. 6 shows the orbits of the $1\times$, $2\times$, and synthetic whirls.

When $1\times$ external perturbing torque is replaced by $2\times$ one, the response amplitudes excited by the $2\times$ perturbing torque ($T = 5000\cos 2\Omega t$) along with unbalance force and weight, and the orbits of disk 1 are shown in Fig. 7. The response is composed of synchronous (i.e., $1\times$), $2\times$, and $3\times$ whirls. Figs. 8 and 9 show the response amplitude of the angle of twist and whirling orbits, respectively. Similar to the symmetric

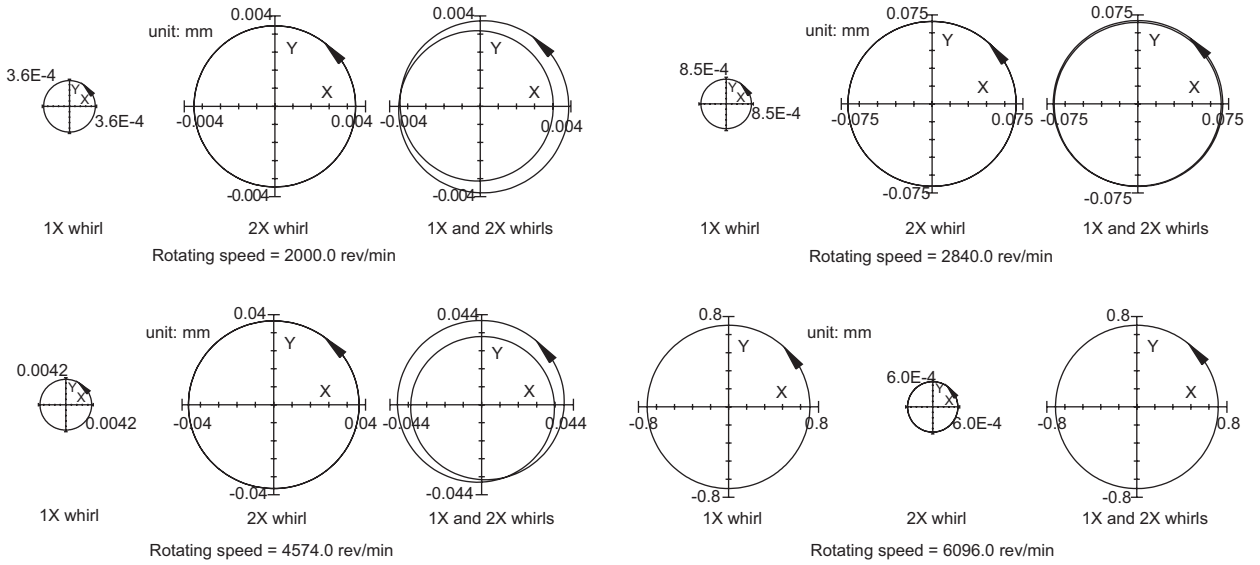

Fig. 6. Whirling orbits of disk 1 ($T = 5000\cos\Omega t$).

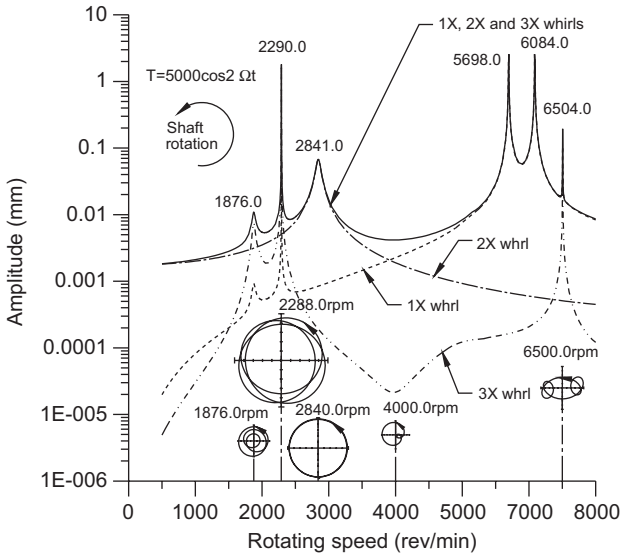

Fig. 7. Response amplitudes and orbits of disk 1 ($T = 5000\cos 2\Omega t$).

isotropic rotor-bearing system [8], a $3\times$ lateral mode in Fig. 7 occurs at 1876.0 rev/min (around one-third of the lateral resonant frequency 5698.0 rev/min) since the $2\times$ perturbing torque excites the $3\times$ forward and $1\times$ backward whirls. Furthermore, a $2\times$ torsional mode occurs at 2290.0 rev/min (see Fig. 8, half of the torsional resonant frequency 4580.0 rev/min) appearing on the $1\times$ and $3\times$ whirl components simultaneously (see Fig. 7). Finally, the $2\times$ and $3\times$ components are excited by weight and the perturbing torque, respectively, their component orbits are forward and right circular (Fig. 9).

5. Conclusion

Due to the impact of the shaft asymmetry, the synchronous lateral mode of asymmetric isotropic rotor-bearing system splits. Different to symmetric system, there exists a $2\times$ lateral mode in the asymmetric system.

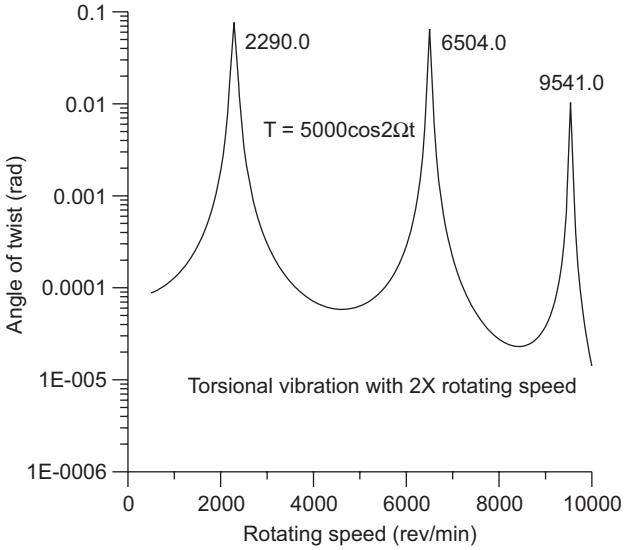

Fig. 8. Angle of twist of disk 1 ($T = 5000\cos 2\Omega t$).

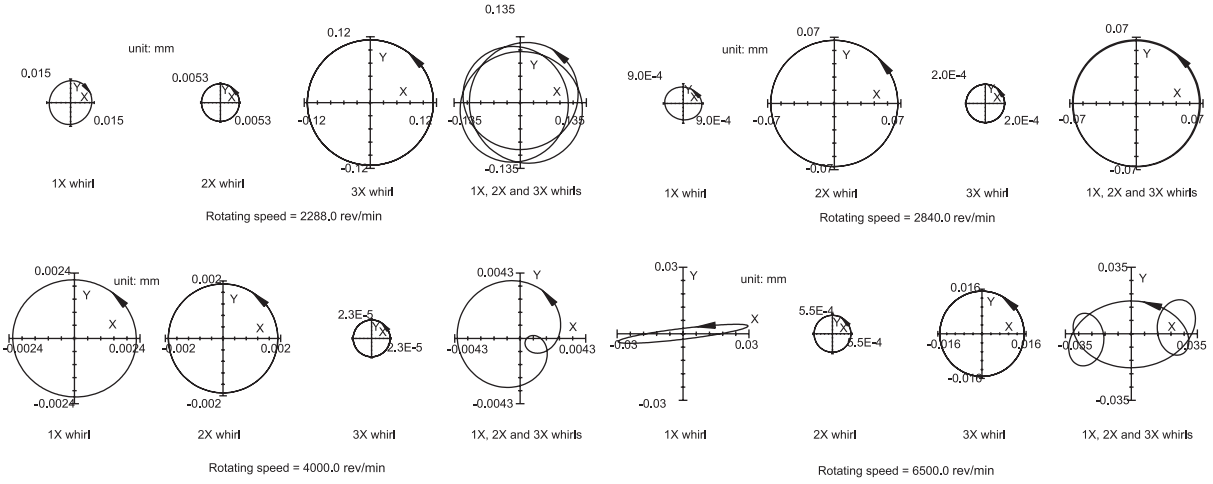

Fig. 9. Whirling orbits of disk 1 ($T = 5000\cos 2\Omega t$).

Unbalance force and weight excited the synchronous whirl and the $2\times$ whirl, respectively. Besides, like the symmetric isotropic rotor-bearing system, the torque will excite the torsional vibration with torsional exciting frequency and, under the system coupling effect, also stimulate the lateral vibration whose frequency is that of the torque plus or minus the rotating speed. In other words, when the unbalance force, weight and the perturbing torque with $n\times$ frequency of the rotating speed simultaneously excite the system, the $(n+1)\times$ forward and $(n-1)\times$ backward whirls appear, along with synchronous and $2\times$ whirls.

References

[1] P. Schwibinger, R. Nordmann, The influence of torsional–lateral coupling on the stability behavior of geared rotor systems, *ASME Journal of Engineering for Gas Turbines and Power* 110 (1988) 563–571.

[2] Q.H. Qin, C.X. Mao, Coupled torsional–flexural vibration of shaft systems in mechanical Engineering—I: finite element model, *Computers and Structures* 58 (1996) 835–843.

[3] J.S. Rao, T.N. Shiau, J.R. Chang, Theoretical analysis of lateral response due to torsional excitation of geared rotors, *Mechanism and Machine Theory* 33 (1998) 761–783.
[4] M.A. Mohiuddin, Y.A. Khulief, Coupled bending torsional vibration of rotors using finite element, *Journal of Sound and Vibration* 223 (1999) 297–316.
[5] B.O. Al-Bedoor, Dynamic model of coupled shaft torsional and blade bending deformations in rotors, *Computer Methods in Applied Mechanics and Engineering* 169 (1999) 177–190.
[6] B.O. Al-Bedoor, Modeling the coupled torsional and lateral vibrations of unbalanced rotors, *Computer Methods in Applied Mechanics and Engineering* 190 (2001) 5999–6008.
[7] C.W. Lee, *Vibration Analysis of Rotor*, Kluwer Academic Publishers, London, 1993.
[8] S.C. Hsieh, J.H. Chen, A.C. Lee, A modified transfer matrix method for the coupling lateral and torsional vibrations of symmetric rotor-bearing systems, *Journal of Sound and Vibration* 289 (2006) 294–333.
[9] Y. Kang, Y.P. Shih, A.C. Lee, Investigation on the steady-state responses of asymmetric rotors, *ASME Journal of Vibration and Acoustics* 114 (1992) 194–208.